Pharmaceutical Research, Vol. 15, No. 4, 1998

Structural and Functional Differences Between Glycosylated and Non-glycosylated Forms of Human Interferon-β (IFN-β)

Laura Runkel[1,2] Werner Meier,[1] R. Blake Pepinsky,[1] Michael Karpusas,[1] Adrian Whitty,[1] Kathleen Kimball,[1] Margot Brickelmaier,[1] Celine Muldowney,[1] Wendy Jones,[1] and Susan E. Goelz[1]

Received November 27, 1997; accepted January 16, 1998

Purpose. Two recombinant IFN-β products have been approved for the treatment of multiple sclerosis, a glycosylated form with the predicted natural amino acid sequence (IFN-β-1a) and a non-glycosylated form that has a Met-1 deletion and a Cys-17 to Ser mutation (IFN-β-1b). The structural basis for activity differences between IFN-β-1a and IFN-β-1b, is determined.

Methods. In vitro antiviral, antiproliferative and immunomodulatory assays were used to directly compare the two IFN-β products. Size exclusion chromatography (SEC), SDS-PAGE, thermal denaturation, and X-ray crystallography were used to examine structural differences.

Results. IFN-β-1a was 10 times more active than IFN-β-1b with specific activities in a standard antiviral assay of 20×10^7 IU/mg for IFN-β-1a and 2×10^7 IU/mg for IFN-β-1b. Of the known structural differences between IFN-β-1a and IFN-β-1b, only glycosylation affected in vitro activity. Deglycosylation of IFN-β-1a produced a decrease in total activity that was primarily caused by the formation of an insoluble disulfide-linked IFN precipitate. Deglycosylation also resulted in an increased sensitivity to thermal denaturation. SEC data for IFN-β-1b revealed large, soluble aggregates that had reduced antiviral activity (approximated at 0.7×10^7 IU/mg). Crystallographic data for IFN-β-1a revealed that the glycan formed H-bonds with the peptide backbone and shielded an uncharged surface from solvent exposure.

Conclusions. Together these results suggest that the greater biological activity of IFN-β-1a is due to a stabilizing effect of the carbohydrate on structure.

KEY WORDS: interferon-β; AVONEX®; Betaseron®; glycosylation; aggregation; activity.

INTRODUCTION

Natural IFN-β is a 166 amino acid glycoprotein that can be produced by most cells in the body in response to viral infection or exposure to other biologics (1,2). It binds to a multimeric cell surface receptor and productive receptor binding results in a cascade of intracellular events leading to the expression of IFN-β inducible genes (3,4). The induction of these genes in turn leads to diverse effects that can be classified through antiviral, antiproliferative, and immunomodulatory activities (4–6). These activities form the basis for the clinical benefits that have been observed with interferon therapy (6,7).

Two very different strategies have been used to generate the two recombinant IFN-β therapeutics, AVONEX® (IFN-β-1a) and Betaseron® (IFN-β-1b), that recently were approved for treatment of multiple sclerosis (8,9). Recombinant IFN-β-1a was expressed in Chinese hamster ovary (CHO) cells to produce a glycosylated form of IFN-β that should be structurally indistinguishable from natural IFN-β in its primary sequence and carbohydrate content (10). Recombinant IFN-β was also expressed as a non-glycosylated protein in E. coli (11). In order to increase yields of biologically active product, the E. coli IFN-β was engineered to carry a Cys-17 to Ser mutation (12) and was later designated as IFN-β-1b because of this change in sequence. The E.coli product also contains a Met-1 deletion as a result of the method of production. Although both products appear to have similar biological activities (12), the *in vitro* potency of the commercially available E. coli product is lower (8,9, see below). While both products have been extensively characterized, they have not been tested side by side in a comparative study and the nature of the structural properties underlying the large differences in potency is unknown.

Here we addressed these issues using clinical lots of AVONEX® (IFN-β-1a) and Betaseron® (IFN-β-1b). In all *in vitro* activity assays performed, IFN-β-1a was at least 10 times more potent than IFN-β-1b. Through systematic evaluation of the potential effects of each of the structural differences on function, we infer that the greater in vitro potency of IFN-β-1a is due to a stabilizing effect of the carbohydrate on structure.

MATERIALS AND METHODS

IFN Preparations

Commercial vials of AVONEX® (Biogen, Inc.; Cambridge, MA) were used in experiments requiring formulated IFN-β-1a. Vials were reconstituted as described on the package insert immediately prior to use. Nonformulated drug in 100 mM sodium phosphate, 200 mM NaCl, pH 7.2 was used in studies requiring purified IFN-β-1a. Commercial vials of Betaseron® (Lot numbers MBAPK024 and MBAPK073; Berlex, Richmond, CA) were used in all experiments with IFN-β-1b. Vials were reconstituted with the supplied diluent as prescribed on the package insert or with PBS immediately prior to use.

Antiviral Activity Assays

The antiviral activity of IFN samples was tested on A549 cells that had been exposed to encephalomyocarditis (EMC) virus. Two versions of the assay were used: a GMP format described in detail in the paper by Alam and coworkers (13) in which samples were tested in two independent experiments by two different analysts for a total of 12 data points and a simpler format for more routine testing in which samples were tested in triplicate. For the latter assay, A549 cells (1.5×10^4 cells/100 μl/well) were plated into 96 well plates. The following day serial dilutions of IFN-β test samples were added, and 24 h later the cells were challenged with EMC virus. Viable cells were quantified two days after viral challenge using the metabolic dye XTT (2,3-bis[2-Methoxy-4-nitro-5-sulfo-phenyl]-2H-tetrazolium-5-carboxyanilide) (14). Cell viability was assessed from absorbance at 450 nm (OD_{450}). One laboratory unit is defined as the IFN-β concentration conferring 50% protection from viral killing (50% maximum OD_{450}).

[1] Biogen, Inc., 14 Cambridge Center, Cambridge, Massachusetts 02142.
[2] To whom correspondence should be addressed. (e-mail: LauraRunkel@Biogen.com)

0724-8741/98/0400-0641$15.00/0

Antiproliferative Activity Assay

The antiproliferative activity of IFN-β was evaluated using the Daudi human B cell line. Cells were maintained at 37°C in a tissue culture incubator in RPMI-1640 medium supplemented with 2 mM glutamine and 10% heat inactivated fetal bovine serum. Cultures of 10^4 cells/well in a 96-well plate were incubated for 40–48 h with serial dilutions of IFN-β. ^{3}H-thymidine (1 μCi in 50 μl medium/well) was added for the final 6 h of incubation and the cultures were then harvested using an LKB Wallac MackII96 automated cell harvester. Thymidine incorporation was measured by scintillation counting. Samples were tested in duplicate.

Assessing Immunomodulatory Function

MHC class I induction by IFN-β was tested using A549 cells. Cells were maintained at 37°C in Dulbecco's modified Eagle's media supplemented with 10% FBS, 2 mM glutamine. Subconfluent cultures (1×10^5 cells/ml) were incubated for 48 h with serial dilutions of IFN-β. The cells were harvested by treatment with 5 mM EDTA in Hank's buffered salt solution, collected by centrifugation, and resuspended at 2×10^7 cells/ml in FACS buffer. MHC Class I expression was assessed by FACS analysis using biotin-conjugated anti-HLA ABC antibodies (Chromaprobe, Inc.) and fluorescein-conjugated streptavidin (Antigenix America). Samples were tested in duplicate.

Preparation of des-1 IFN-β-1a

A recombinant form of the methionine-specific amino peptidase from Salmonella typhimurium was expressed in E. coli and purified as previously described (15). Parallel aliquots of IFN-β-1a (250 μg/ml) in PBS, 0.5 mM $CoCl_2$ were incubated at 30°C for 60 min in the presence or absence of the amino peptidase at an enzyme to substrate ratio of 1:36. For structural studies, the reaction was terminated with EDTA. The Salmonella aminopeptidase was highly specific for removal of Met-1 and only the des-1 cleavage product was detected. Greater than 90% of the Met-1 was removed. For activity measurements, samples were diluted to 4 μg/ml in PBS plus 5% FBS.

Preparation of Deglycosylated IFN-β-1a

IFN-β-1a (250 μg/ml) in 100 mM Na_2HPO_4, 200 mM NaCl pH 7.2 was treated with 0.1 U PNGase F (Oxford Glycosystems) per μg of IFN-β at 37°C. Samples were taken at 24 h time points over a five day period. Deglycosylation was monitored by SDS-PAGE. After PNGase F treatment, insoluble product was removed by centrifugation (15 min, 13,000 rpm). The supernatant was filtered and the concentration of soluble IFN-β-1a determined by absorbance at 280 nm. For activity measurements, the samples were diluted with 15 mg/ml HSA, 0.2 μm filtered, and immediately assayed. While we saw no change in in vitro potency of the des-1 and untreated IFN-β-1a even after a month of storage at 4°C, the deglycosylated IFN-β-1a and SEC samples described below were analyzed without storage to minimize potential changes that might occur over time. Biochemical analyses were also performed on freshly prepared samples.

Preparation of the Cys-17 to Ser Mutation

Site directed mutagenesis was performed by polymerase chain reaction (PCR) amplification of the wild type gene obtained from K562 cell genomic DNA with a 5′ primer encoding the Cys-17 to Ser mutation (GGTGGTCTCACATGAGCTACAACTTGCTTGGATTCCTACAAAGAAGCAGCA ATTTTCAGTCTCA GAAGCTCC) and a wild type 3′ PCR primer. The Cys-17 to Ser mutation was confirmed by DNA sequencing. The PCR fragment was ligated into vector EAG347 (Biogen, Inc.), which contains the simian virus 40 early and adenovirus major late promoters, and the human vascular cell adhesion molecule-1 signal sequence. The wild type IFN-β-1a and Ser-17 mutant genes were electroporated into CHO cells and transiently expressed. Conditioned medium was harvested 3 days post-transfection. IFN-β levels were quantified by ELISA and confirmed by Western blot analyses.

Size Exclusion Chromatography

Samples (0.5 ml) were subjected to sizing at ambient temperature on a TSKG2000SW$_{XL}$ (5 micron) column (7.8 i.dia. × 300 mm; TosoHaas). The chromatography was carried out in 100 mM Na_2HPO_4, 200 mM NaCl pH 7.2 at a flow rate of 1 ml/min and 0.75 ml fractions collected. IFN-β levels in elution fractions were assessed by subjecting samples to SDS-PAGE, staining the gels with Coomassie blue, and then integrating the IFN-β band by densitometry. Enriched preparations of IFN-β-1b aggregate and monomer were generated by running, pooling, and then rechromatographing the appropriate fractions on the same column. Quantitation of IFN-β in the relevant final preparations was complicated by contamination with residual HSA. IFN concentrations were estimated from absorbance measurements at 280 nm using molar extinction coefficients of 30,040 and 41,619 L mol^{-1} cm^{-1} for human IFN-β and HSA, respectively, after adjusting for relative amounts of HSA and IFN-β in the samples by SDS-PAGE analysis. For activity measurements, test samples were diluted with 15 mg/ml HSA, 0.2 μm sterile filtered, and immediately assayed.

SDS-PAGE

Test samples were diluted with reducing electrophoresis sample buffer, boiled for 5 min and analyzed on 10–20% SDS-PAGE gradient gels (Daiichi, 8×10 cm). Protein bands were either directly visualized by Coomassie Brilliant Blue staining or subjected to Western analysis. For Western blotting, proteins were transferred to nitrocellulose and probed with the anti IFN-β mAb BI05 at 0.3 μg/ml (the BI05 antibody was raised against recombinant human IFN-β-1a). Immunoreactive bands were visualized with a goat anti-mouse HRP conjugate using the ECL chemiluminescence kit from Amersham.

Thermal Denaturation Studies

Thermal denaturation of IFN-β was carried out using a CARY 3 UV-visible spectrophotometer fitted with a computer-controlled, thermoelectrically-heated cuvette holder. Solutions of IFN-β in 100 mM Na_2HPO_4, 200 mM NaCl, pH 7.2 were equilibrated at 25°C for 15 min in a 200 μl microcuvette. The temperature of the cuvette holder was then ramped from 25°C to 90°C at a rate of 2°C/min, and the denaturation of the protein

was followed by continuous monitoring of absorbance at 280 nm. The mid-point of the cooperative unfolding event, T_m, was obtained from the melting curves by determining the temperature at which the measured absorbance was mid-way between the values defined by lines extrapolated from the linear regions on each side of the cooperative unfolding transition.

RESULTS

An accurate assessment of the relative in vitro potencies of AVONEX® (IFN-β-1a) and Betaseron® (IFN-β-1b) was made by directly comparing the products in an antiviral CPE assay. In this assay, which utilized A549 cells, EMC virus and WHO natural IFN-β standard (NIH Cat. #Gb23-902-531), specific activities of 20×10^7 IU/mg and 2×10^7 IU/mg were obtained for IFN-β-1a and IFN-β-1b, respectively (Table I). The slightly lower specific activity measured for Betaseron® (2×10^7 IU/mg) compared to the 3.2×10^7 IU/mg previously reported (9) presumably reflects the use of different IFN-β standards. When both products were titered against the WHO recombinant standard (NIH Cat. # Gxb02-901-535) that had been used for Betaseron® (9), AVONEX® had a specific activity of 32×10^7 IU/mg and Betaseron® had the reported specific activity of 3.2×10^7 IU/mg (data not shown). Thus despite the apparent changes in specific activity, the 10-fold difference in potency was maintained.

Since the interferons are multifunctional proteins, and antiviral activity is only one of their known functions, we also examined the relative potencies of IFN-β-1 a and IFN-β-1b in antiproliferative and immunomodulatory assays. Similar activity differences were observed in these assays as well. In the antiproliferative assay, which measured Daudi cell growth by ^{3}H-thymidine incorporation, IC_{50}s of 25 and 300 pg/ml were obtained for IFN-β-1a and IFN-β-1b (Fig. 1A), while in a FACS assay measuring IFN-inducible expression of MHC Class I on the surface of A549 cells, 50% responses were observed at approximately 200 and 3000 pg/ml, respectively (Fig. 1B).

A series of biochemical studies were designed to test if the lack of glycosylation, the Met-1 deletion, or the Cys-17 to Ser mutation could account for the lower in vitro potency of Betaseron®. In these studies, the role of glycosylation and of the Met-1 deletion were directly assessed through enzymatic modification of IFN-β-1a using PNGase F to remove the carbohydrate and using a methionine-specific amino peptidase to remove Met-1. Evaluation of the Cys-17 to Ser mutation required a new DNA construct that was then expressed in CHO cells.

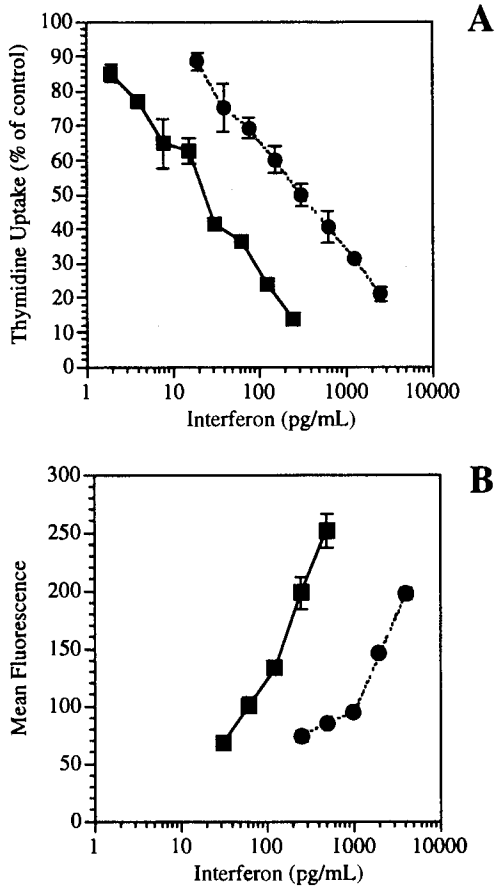

Fig. 1. Antiproliferative and immunomodulatory activities of AVONEX® and Betaseron®. The relative in vitro potencies of IFN-β-1a and IFN-β-1b were measured in an antiproliferative (A) and immunomodulatory assay (B). For measuring antiproliferative activity, subconfluent cultures of Daudi cells were incubated for 2 days with test samples, then labeled with ^{3}H-thymidine, and thymidine incorporation measured by scintillation counting. For measuring immunomodulatory effects, subconfluent cultures of A549 cells were incubated for 2 days with test samples and the induction of MHC class I expression quantified by FACS analysis. AVONEX® (■). Betaseron® (●).

Table I. Specific Activity Measurements in the Antiviral Assay. Data Obtained from GMP Validated Antiviral CPE Assay Were Used to Determine the Specific Activities of Clinical Lots of AVONEX® (IFN-β-1a) and Betaseron® (IFN-β-1b), des-1 IFN-β-1a Prepared by Enzymatic Digestion with S. Typhimurium Amino Peptidase M, and a (−) Enzyme IFN-β-1a Control Subjected to the Same Digestion Conditions but Without Added Enzyme (des-1 Control). The Numbers Presented Are the Mean of 12 Determinations with a Confidence Interval of 95%

Test sample	Specific activity in MU/mg
IFN-β-1a	200
IFN-β-1b	20
des-1 IFN-β-1a	200
des-1 control	210

Treatment of IFN-β-1a with the amino peptidase resulted in the specific removal of Met-1. No aberrant cleavage products were detected. Extensive characterization of the des-1 product by circular dichroism, thermal denaturation studies, and analysis of the disulfide structure (data not shown) revealed that Met-1 removal did not affect secondary and tertiary structure of IFN-β. By SEC, the protein migrated as a monomer. When the des-1 form was compared to wild type IFN-β-1a in the antiviral, antiproliferative and immunomodulatory assays, the Met-1 deletion had no effect on function (see Table 1, Fig. 2 and Fig. 3).

Similarly, changing Cys-17 to Ser and expressing the protein in mammalian cells also had no effect on function (Fig. 3). In this study the Ser-17 mutant and wild type IFN-β-1a genes were transiently expressed in CHO cells. The recombinant products were titered by ELISA and then tested for function

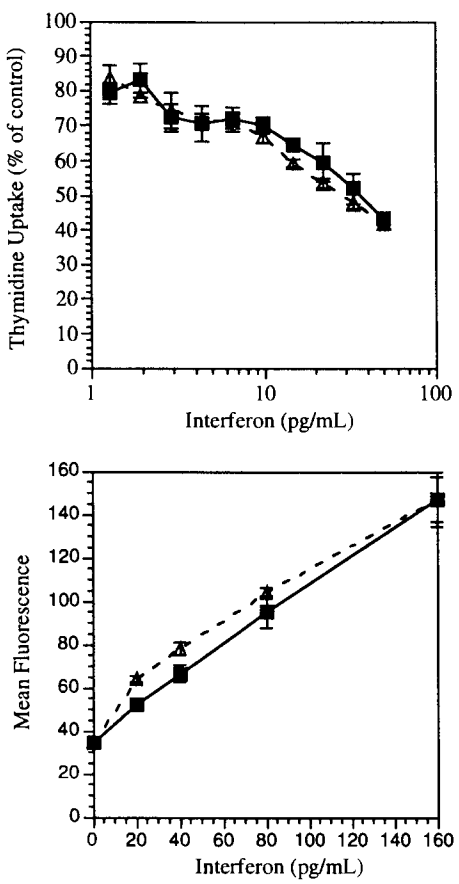

Fig. 2. Characterization of the functional activities of des-1 IFN-β-1a. The relative in vitro potencies of des-1 IFN-β-1a prepared by enzymatic digestion with S. typhimurium amino peptidase M, and of a (−) enzyme IFN-β-1a control subjected to the same digestion conditions but without added enzyme were evaluated in the antiproliferation assay on Daudi cells (A) and in the immunomodulatory assay on A549 cells (B) as described in Fig. 1. (△) enzyme IFN-β-1a control (■). Des-1 IFN-β-1a (△).

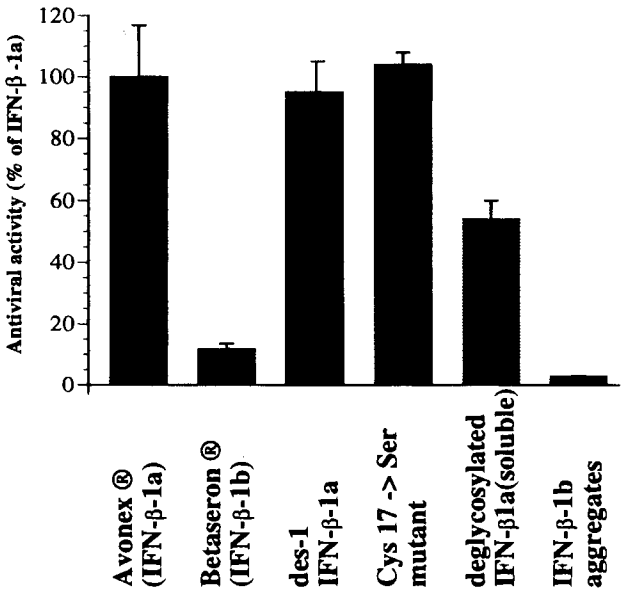

Fig. 3. Comparative analysis of antiviral data. The relative specific activities of IFN-β-1a, des-1 IFN-β-1a, the Cys-17 to Ser mutant, deglycosylated IFN-β-1a, IFN-β-1b, and IFN-β-1b aggregates were evaluated in the antiviral assay. The data are presented as a percent of IFN-β-1a activity: for AVONEX® IFN-β-1a reflecting 100% activity (n = 10), for Betaseron® IFN-β-1b (n = 10), des-1 IFN-β-1a (n = 9), ser- 17 IFN-β-1a (n = 2), deglycosylated, soluble IFN-β-1a (n=2) and IFN-β-1b aggregates (n=3).

using the titer values obtained to determine dilutions for evaluating activity in the antiviral assay.

The role of carbohydrate on IFN-β-1a function was assessed by deglycosylating IFN-β-1a with PNGase F and then comparing it to protein carried through the same treatment but without enzyme. As shown in Fig. 4, PNGase F treatment resulted in a decrease in molecular weight that could be monitored by SDS-PAGE. Deglycosylation by PNGase F was confirmed by electrospray ionization mass spectrometry. The measured mass of 20025 Da matched the predicted mass for non-glycosylated IFN-β-1a starting with Met-1 and terminating with Asn-166 (calculated mass of 20027.1 Da). No loss of carbohydrate occurred in the (−) enzyme control. As had been previously observed (16), a precipitate formed as the sample became deglycosylated that was readily apparent by an increase in sample turbidity. The precipitate was collected by centrifugation and analyzed by SDS-PAGE under reducing and non-reducing conditions (see Fig. 4, lanes 6, 9 and 10). Under reducing conditions, the precipitate migrated as a single band with the predicted mass of non-glycosylated IFN-β (lane 6). In contrast, analysis by non-reducing SDS-PAGE showed that

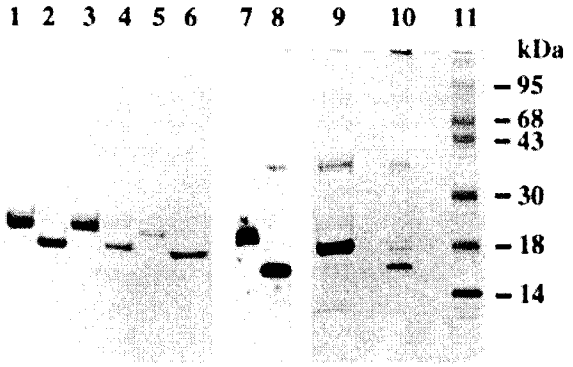

Fig. 4. Characterization of deglycosylated IFN-β-1a by SDS-PAGE. PNGase F treated IFN-β-1a and a (−) enzyme control were fractionated by centrifugation into soluble and precipitated product, subjected to SDS-PAGE under reducing conditions (lanes 1–6, and 9), and visualized by staining with Coomassie blue. Selected samples were analyzed under non-reducing conditions (lanes 7, 8, and 10). Lanes 1, 3, and 5; total, supernatant and pellet fractions, respectively from the (−) enzyme control. Lanes 2, 4, 6: the corresponding fractions from PNGase F treated IFN-β-1a. PNGase F treated IFN-β-1a precipitate under reducing (lane 9) and non-reducing conditions (lane 10). Lane 11, Gibco-BRL prestained high molecular weight markers. Lanes 1–10 were loaded with equivalent amounts of IFN-β. The samples shown in lanes 1–6 were characterized in the antiviral CPE assay, while those shown in lanes 9–10 were from a separate digestion. The small amount of IFN-β dimer seen in lane 9 is due to incomplete reduction. AVONEX® (lane 7) and Betaseron® (lane 8) were directly analyzed by SDS-PAGE/Western blotting under non-reducing conditions.

the precipitate was largely made up of disulfide linked complexes (Fig. 4, lane 10). It was interesting that only the deglycosylated form of IFN-β-1a precipitated (Fig. 4, lanes 3–6). This result was particularly striking at earlier time points where the digestion contained a mixture of intact and deglycosylated product (data not shown). Antiviral activity of the PNGase F treated samples was reduced by about 3-fold, whereas no loss of activity was observed in the (−) enzyme control.

In addition to the deglycosylated IFN-β that had precipitated, about 40% was recovered as a soluble fraction, i.e. that remained in solution after centrifugation and filtration. Reducing SDS-PAGE analysis indicated that the soluble fraction also was fully deglycosylated (see Fig. 4, lane 4). Non-reducing SDS-PAGE showed an absence of the covalent aggregates that were seen in the precipitate. The slightly faster electrophoretic mobility of the IFN-β under non-reducing as compared to reducing conditions is consistent with the product having retained the correct Cys-31 - Cys-141 disulfide bond. The physical state of the soluble fraction was further analyzed by sedimentation velocity ultracentrifugation and circular dichroism. By analytical ultracentrifugation, over 95% of the protein migrated as a monomer with an average sedimentation coefficient of 1.73. Under the same conditions, untreated IFN-β-1a and the minus enzyme control migrated at 1.91 S and 1.99 S, respectively. Circular dichroism spectra for the same three samples were indistinguishable, indicating that deglycosylation had not caused any gross change in the secondary and tertiary structure of the IFN-β-1a (data not shown). In addition to the biochemical studies, the soluble fraction of the PNGase F digested IFN-β-1a was also analyzed for function in the antiviral, antiproliferative, and immunomodulatory assays. As shown in Fig. 3, the deglycosylated soluble fraction had only a slightly lower specific activity than the (−) enzyme control in the antiviral assay. Similarly, a 2 fold drop in the specific activity of the deglycosylated IFN-β-1a was observed in the antiproliferative assay and a 1.4 fold drop in its specific activity in the immunomodulatory assay (data not shown). Thus, while removal of the carbohydrate moiety *per se* does not account for the observed 10 fold specific activity differences between IFN-β-1a and IFN-β-1b (Fig. 3), the decreased solubility of the deglycosylated IFN-β-1a and decrease in total activity due to aggregation suggest an indirect involvement.

Independent evidence on the effect of aggregation on the activity of IFN-β was obtained by SEC. When Betaseron® was subjected to SEC under physiological conditions, approximately 40% of IFN-β-1b eluted as monomer and 60% eluted in the excluded volume of the column with an apparent molecular weight of >600 kDa (Fig. 5). The aggregated IFN-β-1b migrated as monomer by non-reducing SDS-PAGE indicating that the complexes were non-covalent (data not shown). In contrast, when IFN-β-1a was subjected to SEC using the same conditions, greater than 98% of the IFN-β-1a was monomeric (Fig. 5). Since aggregate formation can be buffer dependent and since it is known that certain chromatography matrices can perturb the physical state of some proteins, the two products were also analyzed using different buffers and different columns (data not shown). The results were the same. As part of the characterization, the IFN-β-1b monomer and aggregate peaks were rechromatographed and the resulting pools analyzed for antiviral activity. The specific activity of the IFN-β-1b aggregate was 3-fold lower than the starting material (0.7×10^7 IU/mg versus 2×10^7 IU/mg). Accurate estimates of the IFN-β-1b monomer specific activity could not be determined because each time the preparation was rechromatographed the product reequilibrated to form a mixture of monomer and aggregate. In contrast, the IFN-β-1a monomer peak rechromatographed as a monomer and the specific activity of the resulting product was equivalent to the starting material.

The three dimensional structures of interferons are similar, raising the possibility of using available crystallographic data to gain insights into the differences in *in vitro* potency of IFN-β-1a and IFN-β-1b. In an attempt to understand what effect the carbohydrate might have on activity and/or structure, we compared crystallographic data for IFN-β-1a (AVONEX®) (17) as an example of glycosylated IFN and of IFN-α-2b (18) as an example of a naturally non-glycosylated IFN. Results from this analysis are presented in Fig. 6, top panel. In the AVONEX® structure, the glycan shields an uncharged surface that is made up exclusively of hydrophobic and polar amino acids. In the IFN-α-2b structure, Lys-83 and Arg-22 introduce charged residues at the exact positions in the AVONEX® structure that are hydrogen-bonded to the core glycan through uncharged, polar amino acid residues (Fig. 6, bottom panel). Moreover, Asn-80 in IFN-β is replaced with an aspartic acid in IFN-α-2b. Thus, while the glycan shielded surface of IFN-β is uncharged, the corresponding region in the naturally non-glycosylated IFN-α molecule is not. In IFN-β-1a, removal of the glycan would expose this uncharged surface to solvent which would be thermodynamically unfavorable and might account for the propensity of the non-glycosylated protein to aggregate. In IFN-α-2b, which is naturally non-glycosylated, charged residues substitute for the glycan contact points, reducing the hydrophobic character of the surface.

A surprising feature of the AVONEX® structure was that a significant portion of the glycan and contacts between the glycan and the peptide backbone were visible. This is highly unusal for a glycoprotein, since in most structures that have been solved the glycan is usually unordered. In the AVONEX® structure, the fucosylated trimannosyl core sugars plus an additional hexose attached to Asn-80 were visible with the glycan protruding outward from the N-terminal end of the C-helix. Only minimal contact occurs between the glycan and other parts of the protein. Fig. 6, bottom panel, shows an enlargement of this region of the structure. Two H-bond contacts were identified between the core α1-6 fucose residue and the side chains of Asn-86 (in helix-C) and Gln-23 (in helix-A). The presence of these contacts suggested that the carbohydrate might play a direct role in stabilizing the IFN-β structure. To test this possibility soluble, deglycosylated IFN-β-1a and a (−) enzyme control that had been treated identically were subjected to thermal denaturation, using the point at which a protein denatures due to thermal stress as a measure of stability. Results from this analysis are shown in Fig. 7. At a protein concentration of 100 μg/ml, deglycosylated IFN-β-1a denatured at T_m = 62.9±0.3°C, while the control IFN-β-1a with carbohydrate denatured at T_m = 67.3±0.3°C. In this type of study, a shift of 4–5°C in the point at which the IFN-β denatures is highly significant. While the temperature needed to induce denaturation was somewhat dependent on protein concentration (see Fig. 7), the difference between the control and deglycosylated protein remained constant across all protein concentrations tested. This consistent difference in thermal stability supports

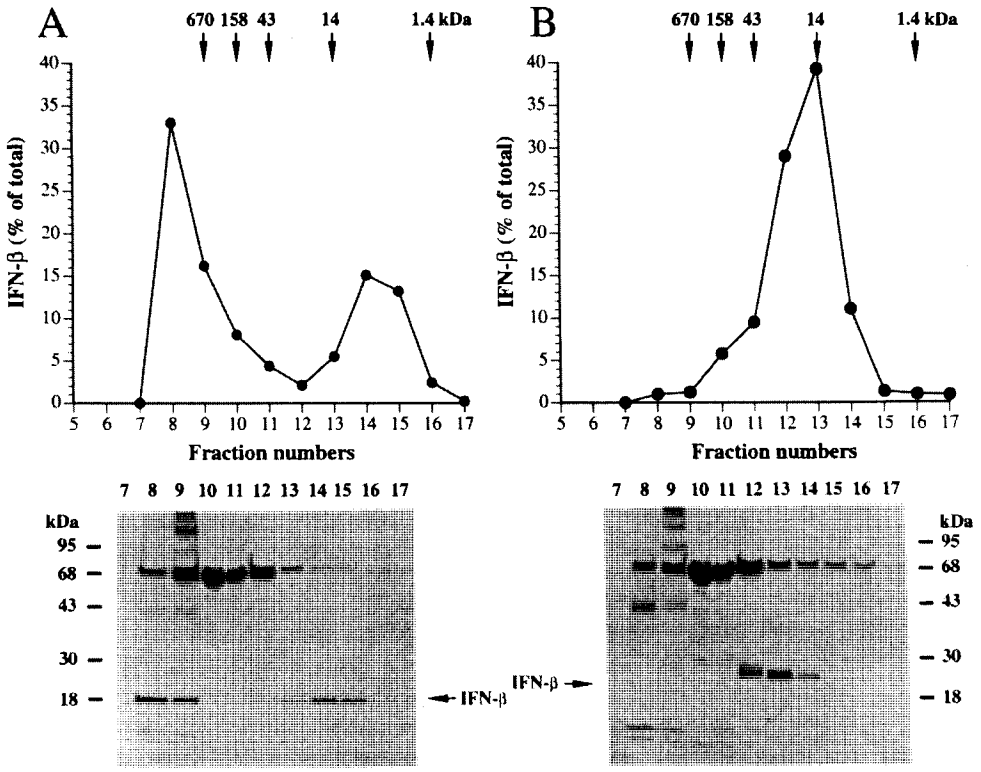

Fig. 5. Analysis of IFN-β-1a and IFN-β-1b by SEC. IFN-β-1b (A) and IFN-β-1a (B) were subjected to SEC on a TSKG2000SW column using 100 mM sodium phosphate, 200 mM NaCl pH 7.2 as the mobile phase. The column effluent was monitored for absorbance at 280 nm. Column fractions (15 μl aliquots for fractions 7–9 and 12–17, 1.5 ul for fractions 10–11) were subjected to SDS-PAGE under reducing conditions and visualized by Coomassie blue staining (bottom panel). The top panel shows a graphic representation of the elution data where the IFN-β bands from the SDS-PAGE were integrated by densitometry and plotted for each fraction as a percentage of the total IFN-β recovered. The elution positions of column standards are indicated at the top.

the notion that the change in the temperature of denaturation is due to stabilization of the IFN-β structure by the sugar.

DISCUSSION

We have directly compared the relative *in vitro* potencies of AVONEX® (IFN-β-1a) and Betaseron® (IFN-β-1b) in functional assays and showed that the specific activity of IFN-β-1a is 10–15 fold greater than the specific activity of IFN-β-1b. From studies designed to identify the structural basis for these activity differences, glycosylation was the only one of the known structural differences between the products that affected function. The effect of the carbohydrate was largely manifested through its stabilizing role on structure. Lack of glycosylation was correlated with an increase in aggregation and an increased sensitivity to thermal denaturation.

Enzymatic removal of the carbohydrate from IFN-β-1a with PNGase F caused extensive precipitation of the deglycosylated product. An unexpected feature of the precipitate was that a large fraction had undergone disulfide interchange as evidenced by the presence of high molecular weight disulfide linked complexes that were detected by non-reducing SDS-PAGE but not under reducing conditions. No disulfide-linked complexes were seen in the controls subjected to the same digestion conditions but without PNGase F. Since all of the cysteine residues in IFN-β are normally buried (16), the data imply that deglycosylation has caused a large fraction of the protein to denature. While the denaturation process is not understood, the disulfide scrambling is similar to that described previously by others working with the wild type IFN-β produced in E. coli (12). Activity data could not be obtained for the insoluble precipitate; however, previously published data showed and we had also noted (data not shown) that IFN-β aggregates had reduced biological activity (12).

When thermal denaturation experiments were performed on the soluble fraction after PNGase F treatment and the (−) enzyme control, the loss of carbohydrate resulted in a 4–5°C shift in the point of denaturation. This type of response indicates that the energy of stabilization that is provided by the carbohydrate is large. Thermal denaturation was irreversible at both low and high protein concentrations, and at the higher concentrations, melting caused the protein solutions to become turbid, presumably as a result of the formation of insoluble aggregates.

The stabilizing effect of the carbohydrate was also evident from SEC analysis. Under physiological conditions, AVONEX® eluted as a monomer, while a large fraction of the Betaseron® product eluted as soluble aggregates that had reduced antiviral activity. The propensity of IFN-β-1b to aggregate suggests a very different solubility profile of IFN-β-1a and IFN-β-1b.

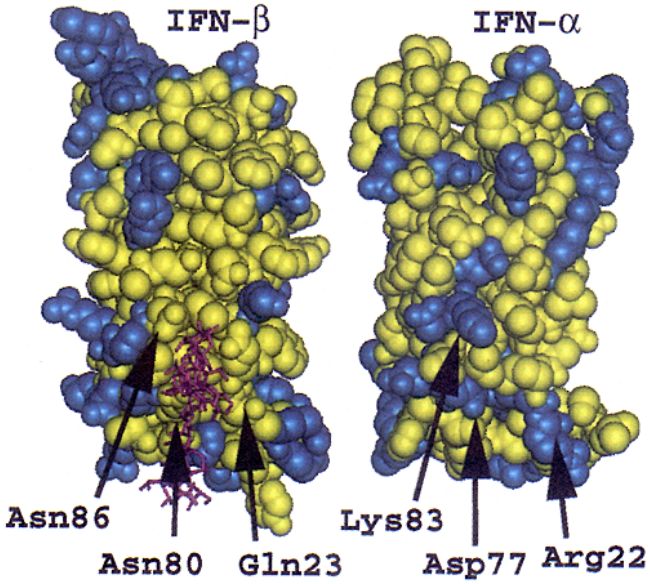

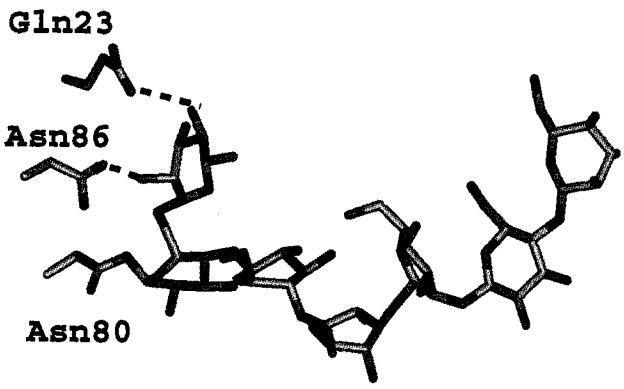

Fig. 6. Alignment of the structures of IFN-β-1a and IFN-α-2b. The crystal structure of IFN-β-1a (17) and the homology model of IFN-α-2b (18) were superimposed and the region corresponding to where the glycan is attached in human IFN-β positioned at the front. To better highlight the key structural features of this region, the structures were then separated and presented side by side using space filling models for the peptide backbone and a stick model for the glycan core in purple (top panel). Charged amino acids are colored blue and the rest are colored yellow. An enlargement of the IFN-β-1a structure showing contacts between the glycan and protein side chains (bottom panel).

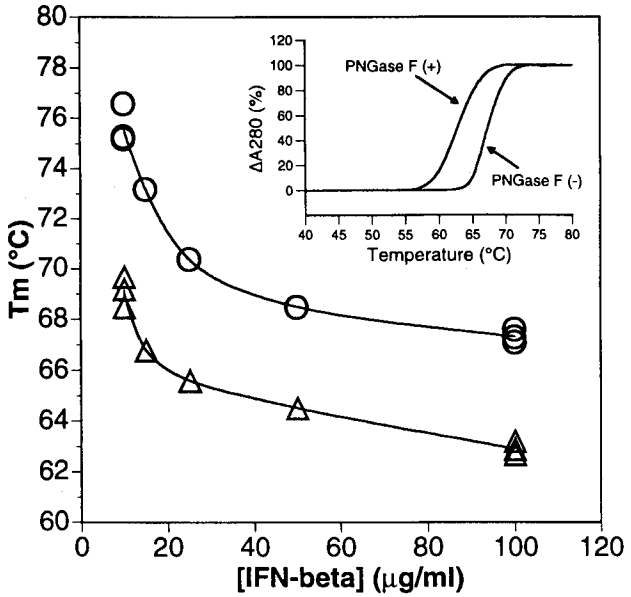

Fig. 7. Characterization of deglycosylated IFN-β-1a by thermal denaturation. PNGase F treated IFN-β-1a (△) and a (–) enzyme control (○) in 100 mM Na_2HPO_4, 200 mM NaCl pH 7.2 were heated at a fixed rate of 2°C/min. Denaturation was following by monitoring the absorbance change at 280 nm. Melting temperature T_m was determined from the melting curves and plotted as a function of IFN-β concentration as described in the experimental section. The insert plot shows actual melting curves observed at a protein concentration of 100 μg/ml.

Crystallographic data also suggested a stabilizing effect of the carbohydrate. While published crystal structures for a non-glycosylated form of murine IFN-β (19) and for human IFN-α-2b (20), which is naturally non-glycosylated, had provided models for the polypeptide backbone of human IFN-β, the recently solved structure for AVONEX® in its glycosylated state (17) provided a first glimpse of the spatial orientation of the glycan with respect to the remainder of the structure. In the AVONEX® structure, specific contacts between the glycan and the A- and C-helices on the peptide backbone indicated that the carbohydrate directly stabilized the IFN-β structure. Further inspection of the structure revealed that the glycan structure minimized solvent exposure of an uncharged surface with an abnormally large number of hydrophobic amino acids; such exposure would be thermodynamically unfavorable in non-glycosylated forms of IFN-β. Aggregation of unglycosylated IFN-β might represent a mechanism for protecting this surface from the aqueous environment, which in turn could explain the precipitation seen with PNGase F treatment of IFN-β-1a. It was interesting that the exact residues in IFN-β that make contact with the glycan are charged residues in IFN-α (Fig. 6). The crystallographic data highlight how two closely related proteins evolved different mechanisms to deal with this region of the structure.

While there is no available crystallographic data for human IFN-β-1b, the published crystal structure of murine IFN-β provides interesting insights into the structure of a non-glycosylated form of IFN-β. Although natural murine IFN-β has two glycosylation sites, one of which corresponds to Asn-80, the murine crystal structure is of a non-glycosylated E. coli-derived product. Despite sequence differences between the human and mouse proteins, the secondary and tertiary structures in the relevant region of the Asn-80 glycosylation are superimposable in the two crystal structures, indicating that the three dimensional structures of glycosylated and non-glycosylated human IFN-β may be similar. However, the analogy is weakened by the fact that the murine and human sequences differ in two important ways. First, Asn-86 is replaced with an arginine in the murine sequence, making the hydrophobicity of the normally glycan shielded surface of murine IFN-β somewhere between that of human IFN-β and IFN-α, and potentially more soluble. In fact in the murine study (21), the authors comment on having attempted but failed to crystallize non-glycosylated human IFN-β expressed in E. coli. Second, the murine sequence lacks two of the three Cys residues found in human sequence, which

would eliminate the possibility of forming high molecular weight covalent complexes through disulfide scrambling.

Since the three cysteine residues in human IFN-β are normally buried (17), disulfide scrambling implies that a denaturation event has occurred. One possibility is that aggregate formation drives the denaturation. In this model, the deglycosylated product would exist in one of two states; either as a soluble monomer as is represented in the murine structure, or as an aggregate. As an aggregate formed, the structure could then rearrange to form the disulfide-linked complexes. The SEC studies performed with IFN-β-1b suggest that the non-glycoslated IFN-β aggregate is at a lower energy state than the monomer since the monomer-aggregate equilibrium favored the formation of aggregate. It is possible that the free Cys residue in deglycosylated IFN-β-1a catalyzes the disulfide scrambling to form an insoluble aggregate, since IFN-β-1b, which lacks the relevant Cys, only forms a soluble aggregate. Further studies are needed to better understand the denaturation event.

For most glycoproteins, the role of the carbohydrate is undefined. Although glycan groups can contribute to the biological activity and pharmacodynamic properties of proteins (22,23), the most common function is structural where they facilitate protein folding and/or stabilize the mature conformation (23–26). The data we and others generated for IFN-β clearly support a stabilizing role of the sugars (16,27). A fundamental difference between the deglycosylated form of IFN-β-1a and nonglycosylated IFN-β-1b is that the IFN-β-1a is folded in its glycosylated state and the sugar is then enzymatically removed, while IFN-β-1b is folded in the absence of carbohydrate. While we have not directly studied the role of carbohydrate on the folding of IFN-β, it is clear from studies with other proteins that the effects of glycosylation on folding and mature structure are often coupled (24–26,28–32). To test for other potential structural differences between IFN-β-1a and IFN-β-1b we compared the thermal stability of these proteins in thermal denaturation experiments. Preliminary data for deformulated IFN-β-1b revealed a T_m of about 12°C lower than that seen for the same concentration of glycosylated IFN-β-1a and was less stable than deglycosylated IFN-β-1a by about 7°C (data not shown). Although the thermal denaturation data show that non-glycosylated IFN-β-1b and deglycosylated IFN-β-1a are different, the method does not address whether the result is due to a difference in folding or stability. More detailed studies aimed at testing the effects of glycosylation on protein folding will be particularly important for IFN-β because of the different strategies that are currently used to make recombinant IFN-β-1a and IFN-β-1b.

ACKNOWLEDGMENTS

We wish to thank Rohin Mhatre, Ling Ling Chen, Lee Walus, Chenhui Zeng, Dingyi Wen, Steve Berkowitz, and the Bioassay group at Biogen for assisting in various studies. Special thanks go to Paula Hochman for support and critical reading of the manuscript.

REFERENCES

1. W. E. Stewart. The interferon system. Springer Verlag, New York (1981).
2. G. Sen and P. Lengyel. The interferon system: a bird's eye view of its biochemistry. *J. Biol. Chem.* **267**:5017–5020 (1992).
3. G. Uze, G. Lutfalla, and K. E. Mogensen. Alpha and beta interferons and their friends and relations. *J. Interferon Cytokine Res.* **5**:3–26 (1995).
4. M. Peters. Actions of cytokines on the immune response and viral interactons: an overview. *Hepatology* **23**:909–916 (1996).
5. S. K. Tyring. Interferons: Biochemistry and mechanisms of action. *Am. J. Obstet. Gynecol.* **172**:1350–1353 (1995).
6. B. Weinstock-Guttman, R. M. Ransohoff, R. P. Kinkel, and R. A. Rudick. The interferons: biological effects, mechanisms of action, and use in multiple sclerosis. *Ann. Neurol.* **37**:7–13 (1995).
7. S. Baron, D. H. Coppenhaver, F. Dianzani, R. Fleischmann, T. K. Hughes Jr., G. R. Klimpel, D. W. Niesel, G. J. Stanton, and S. K. Tyring. Interferon: principles and medical applications. *The University of Texas Medical Branch at Galveston; Dept. of Microbiology.* Galveston, TX (1992).
8. L. D. Jacobs, D. L. Cookfair, R. A. Rudick, R. M. Herndon, J. R. Richert, A. M. Salazar, J/ S Fischer, D. E. Goodkin, C. V. Granger, J. H. Simon, J. J. Alam, D. M. Bartoszak, D. N. Bourdette, J. Braiman, C. M. Brownscheidle, M. E. Coats, S. L. Cohan, D. S. Dougherty, R. P. Kinkel, M. K. Mass, F. E. Munschauer, III, R. L. Priore, P. M. Pullicino, B. J. Scherokman, B. Weinstock-Guttman, R. H. Whitham, and the Multiple Sclerosis Collaborative Research Group. Intramuscular interferon-beta-1a for disease progression in relapsing multiple sclerosis. *Ann. Neurol.* **39**:285–294 (1996).
9. The IFNβ multiple sclerosis study group. Interferon-beta-1b is effective in relapsing-remitting multiple sclerosis. I. Clinical results of a multicenter, randomized, double-blind, placebo controlled trial. *Neurology* **43**:655–661 (1993).
10. Y. Kagawa, S. Takasaki, J. Utsumi, K. Hosoi, H. Shimizu, N. Kochibe, and A. Kobata. Comparative study of the asparagine-linked sugar chains of natural human interferon-β1 and recombinant human interferon -β1 produced by three different mammalian cells. *J. Biol. Chem.* **263**:17508–17515 (1988).
11. R. Derynck, E. Remaut, E. Saman, P. Stanssens, E. De Clercq, J. Content, and W. Fiers. Expression of the human fibroblast interferon gene in *Escherichia coli.* Nature **287**:193–197 (1980).
12. D. F. Mark, S. D. Lu, A. A. Creasey, R. Yamamoto, and L. S. Liu. Site-Specific mutagenesis of human fibroblast interferon gene. *Proc. Natl. Acad. Sci. USA* **81**:5662–5666 (1984).
13. J. Alam, S. Goelz, P. Rioux, J. Scaramuccii, W. Jones, A. McAllister, M. Campion, and M. Rogge. Comparative pharmacokinetics and pharmacodynamic of two recombinant human interferon beta-1a (IFNβ-1a) Products Administered Intramuscularly in Healthy Male and Female Volunteers. *Pharm. Res* **4**:546–549 (1997).
14. L. M. Jost, J. M. Kirkwood, and T. L. Whiteside. Improved short- and long- term XTT-based colorimetric cellular cytotoxicity assay for melanoma and other tumor cells. *J. Immunol. Meth.* **147**:153–165 (1992).
15. P. P. Wingfield, G. Graber, N. R. Turcatti, M. Movva, S. Pelletier, Craig, K. Rose, and C. G. Miller. Purification and characterization of a methionine specific aminopeptidase from Salmonella Typhimurium. *Eur. J. Biochem.* **180**:23–32 (1989).
16. H. S. Conradt, H. Egge, J. Peter-Katalinic, W. Reiser, T. Siklosi, and K. Schaper. Structure of the carbohydrate moiety of human interferon beta secreted by a recombinant Chinese hamster ovary cell line. *J. Biol. Chem.* **262**:14600–14605 (1987).
17. M. Karpusas, M. Nolte, C. B. Benton, W. Meier, W. N. Lipscomb, and S. E. Goelz. The crystal structure of human interferon-β at 2.2 Å resolution. *Proc. Natl. Acad. Sci.* USA **94**:11813–11818 (1997).
18. N. J. Murgolo, W. T. Windsor, A. Hruza, P. Reichert, A. Tsarbopoulos, S. Baldwin, E. Huang, B. Pramanik, S. Ealick, and P. P. Trotta. A homology model of human interferon α-2. *Proteins: Struc., Func., Gen.* **17**:62–74 (1993).
19. T. Senda, S. Saitoh, and Y. Mitsui. Refined crystal structure of recombinant murine Interferon-β at 2.15 Å resolution. *J. Mol. Biol.* **253**:187–207 (1995).
20. R. Radhakrishnan, L. J. Walter, A. Hruza, P. Reichert, P. P. Trotta, T. L. Nagabhushan, and M. R. Walter. Zinc mediated dimer of human interferon-α2b revealed by x-ray crystallography. *Structure* **4**:1453–1463 (1996).
21. Y. Mitsui, T Senda, T.Shimazu, S. Matsuda, and J. Utsumi. Structural, Functional and evolutionary implications of the three-

dimensional crystal structure of murine interferon beta. *Pharmacol. Ther.* **58**:93–132 (1993).
22. T. W. Rademacher, R. B. Parekh, and R. A. Dwek. Glycobiology. *Ann. Rev. Biochem.* **57**:785–838 (1988).
23. J. C. Paulson. Glycoproteins: What are the sugar chains for? *Trends Biochem. Sci.* **14**:272–276 (1989).
24. H. Lis and N. Sharon. Protein glycosylation: structural and functional aspects. *Eur. J. Biochem.* **218**:1–27 (1993).
25. C. Wang, M. Eufemi, C. Turano, and A. Giartosio. Influence of the carbohydrate moiety on the stability of glycoproteins. *Biochemistry* **35**:7299–7307 (1996).
26. S. E. O'Connor and B. Imperiali. Modulation of protein structure and function by asparagine-linked glycosylation. *Chem. and Biol.* **3**:803–812 (1996).
27. Y. Watanabe and Y. Kawade. Properties of non-glycoslated human interferon-β from MG63 cells. *J. Gen. Virol.* **64**:1391–1395 (1983).
28. R. Gibson, S. Schlesinger, and S. Kornfeld. The non-glycosylated glycoprotein of vesicular stomatitis virus is temperature-sensitive and undergoes intracellular aggregation at elevated temperatures. *J. Biol. Chem.* **254**:3600–3607 (1979).
29. S. Dube, J. W. Fisher, and J. S. Powell. Glycosylation at specific sites of erythropoietin is essential for biosynthesis, secretion and biological function. *J. Biol. Chem.* **263**:17516–17521 (1988).
30. D. T. W. Ng, S. W. Hiebert, and R. A. Lamb. Different roles of individual N-linked oligosaccharide chains in folding, assembly, and transport of the simian virus 5 hemmagglutinin-neuraminidase. *Mol. Cell. Biol.* **10**:1989–2001 (1990).
31. D. Davis, X. Liu, and D. L. Segaloff. Identification of the sites of N-linked glycoslyation on the follicle-stimulating hormone (FSH) receptor and assessment of their role in FSH receptor function. *Mol. Endo.* **9**:159–170 (1995).
32. M. E. Mathieu, P. R. Grigera, A. Helenius, and R. R. Wagner. Folding, unfolding and refolding of the vesicular stomatitis virus glycoprotein. *Biochemistry* **35**:4084–4093 (1996).